Planar jumping-drop thermal diodes

Jonathan B. Boreyko, Yuejun Zhao, and Chuan-Hua Chen[a)]
Department of Mechanical Engineering and Materials Science, Duke University, Durham, North Carolina 27708, USA

(Received 28 July 2011; accepted 15 November 2011; published online 9 December 2011)

Phase-change thermal diodes rectify heat transport much more effectively than solid-state ones, but are limited by either the gravitational orientation or one-dimensional configuration. Here, we report a planar phase-change diode scalable to large areas with an orientation-independent diodicity of over 100, in which water/vapor is enclosed by parallel superhydrophobic and superhydrophilic plates. The thermal rectification is enabled by spontaneously jumping dropwise condensate which only occurs when the superhydrophobic surface is colder than the superhydrophilic surface. © *2011 American Institute of Physics*. [doi:10.1063/1.3666818]

Analogous to the electronic diode, a thermal diode transports heat with a strong directional preference. Thermal diodes are useful in a variety of applications, such as heat distribution in spacecrafts,[1] thermal regulation during energy harvesting,[2] thermally adaptive building materials,[3] and potentially phononic computing.[4] The effectiveness of a thermal diode is measured by the rectification coefficient (diodicity),

$$\eta = \frac{k_f - k_r}{k_r}, \tag{1}$$

where k_f and k_r are the effective thermal conductivities in the forward and reverse operating modes, respectively.

Thermal diodes that have been reduced to practice have significant constraints that limit their practical applications. Solid-state thermal diodes[4] can be configured in a variety of form factors and function over a wide range of temperatures, but their diodicity is typically limited to $\eta \sim 1$ or less.[5–7] Phase-change thermal diodes[8] such as thermosyphons[9] and asymmetric heat pipes[1] can produce a diodicity of $\eta \sim 100$. However, thermosyphons are only useful with an orientation favored by gravity, a severe limitation for mobile electronics and space applications, while asymmetric heat pipes are fundamentally one-dimensional, a major constraint for applications requiring planar configurations. Integration of an array of asymmetric heat pipes into a wall panel solves the dimensionality problem but results in an order-of-magnitude decrease in the diodicity.[3]

Here, we report a phase-change thermal diode (Fig. 1) that is inherently planar with an orientation-independent diodicity of $\eta \sim 100$. Instead of relying on gravity or a wick structure to transport the condensate back to the evaporator, our diode is enabled by the self-propelled jumping motion of dropwise condensate on a superhydrophobic surface.[10,11] In the process of condensation, coalescing drops release surface energy which propels the merged drops to jump out-of-plane; the directionality results from the substrate breaking the symmetry of the energy release by exerting a perpendicular force.[12]

The jumping-drop thermal diode consists of a planar vapor chamber with opposing superhydrophobic and superhydrophilic[13] plates (Fig. 1). The plates are separated by a thermally insulating gasket which also provides a vacuum seal. When the superhydrophilic surface is heated with respect to the superhydrophobic one (forward mode, Fig. 1(a)), the evaporating water carries heat away from the superhydrophilic surface and the vapor condenses on the superhydrophobic surface; the self-propelled jumping motion returns the condensed drops back to the evaporator, completing the circulation of working fluid with highly effective phase-change heat transfer. When the superhydrophilic surface is cooler (reverse mode, Fig. 1(b)), liquid water is trapped by it and no phase-change heat transfer takes place; heat mainly escapes through ineffective conduction across the rubber gasket and vapor space. Note that the wick structure in our thermal diode serves to evenly distribute the working liquid *within* the superhydrophilic surface and hold it against gravity. In contrast, the wick in conventional heat pipes is playing the additional role of returning condensate to the evaporator by capillary action.[8]

The superhydrophobic surface (Fig. 2(a)) was fabricated using electroless galvanic deposition of silver nanoparticles onto a copper substrate[14] and was subsequently coated with a monolayer of 1-hexadecanethiol. The superhydrophobic plate had two ports for liquid injection and vacuum pumping (visible in Fig. 2(a) inset). The opposing superhydrophilic surface (Fig. 2(b)) consists of copper wick sintered to a copper plate[15] and oxidized by oxygen plasma. The copper plates had a cross-sectional area of $A = 76\,\text{mm} \times 76\,\text{mm}$, a thickness of 8.9 mm (superhydrophobic) and 6.4 mm (superhydrophilic), and a thermal conductivity of 400 W/m·K. The plate dimensions were somewhat arbitrary and chosen primarily to facilitate fabrication. The copper wick had an area of $A_w = 61\,\text{mm} \times 61\,\text{mm}$, a thickness of $H_w = 1.0\,\text{mm}$, and a conductivity of approximately 40 W/m·K.[15]

The parallel copper plates were separated by a water-resistant rubber gasket (EPDM, 0.1 W/m·K). Through-holes were punched along the gasket to allow for the passage of glass-filled nylon screws (0.2 W/m·K), which were used to seal the chamber air-tight. The compressed thickness of the rubber gasket defined the total separation between the plates, $H = 2.6\,\text{mm}$, and consequently the height of the vapor space, $H_v = 1.6\,\text{mm}$. Once sealed, the injection port was opened to charge 2 mL of deionized water into the chamber, an amount

[a)]Electronic mail: chuanhua.chen@duke.edu.

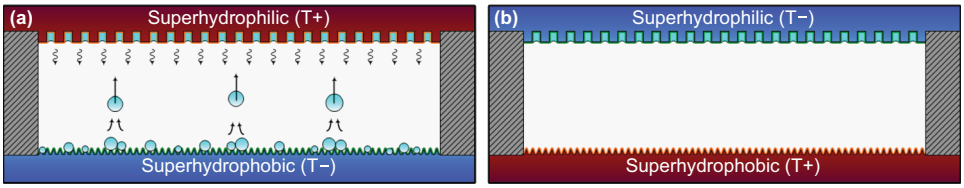

FIG. 1. (Color online) Schematic of the planar jumping-drop thermal diode (not to scale). (a) Forward mode with self-propelled jumping drops returning the working fluid from the superhydrophobic condenser to the superhydrophilic evaporator for continuous phase-change heat transfer and (b) reverse mode with liquid trapped by the colder superhydrophilic surface.

just enough to soak the wick. With both ports closed, the whole chamber was heated to a uniform temperature of 40 °C (to ensure consistent removal of non-condensable gases). The vacuum port was then opened until a chamber pressure of 10 kPa was achieved, at which point both ports were sealed. Subtracting the vapor pressure, the partial pressure of the non-condensable gases in the chamber was estimated to be roughly 3 kPa.

The effective conductivity across the vapor chamber was measured by $k_{eff} = HQ/(A\Delta T)$, where ΔT was the steady-state temperature drop between the copper plates at a given power input Q, and A is the total cross-sectional area of the plates including the surrounding gasket. In the characterization experiments, one copper plate was heated by a resistive film heater (also of area A) at a specified power (Q), while the other was cooled by a chiller plate held at a constant temperature (T_0) by a refrigerated circulator. The backside of the heater was wrapped with insulating rubber foam (0.04 W/m·K, 10 mm thick) to minimize heat leakage. The temperatures were measured using two thermistors (Omega 44131) drilled into the sides of each plate, 2 mm beneath the functional surfaces.

The thermal diode was characterized at three different orientations (Fig. 3(a)): against gravity (superhydrophobic substrate on the bottom, as in Figs. 1, 3(b) and 3(c)), with gravity (on top), and neutral of gravity (sideways), over the course of a week-long continuous run. Within the experimental uncertainties, all three orientations equivalently demonstrate low conductance in the reverse mode and high conductance in the forward mode, verifying a complete orientation independence. Even when the diode chamber was flipped upside down in the middle of a steady-state operation, there was no appreciable change in the measured temperature drop.

The highly effective thermal rectification is illustrated with infrared imaging (FLIR A325) in Figs. 3(b) and 3(c), where a spray paint of known emissivity (Krylon flat white 1502) was applied to the side of the diode. Under identical conditions, steady-state operation in the forward and reverse modes yielded dramatically different temperature distributions. In the forward mode (Fig. 3(c)), the effective phase-change heat transfer led to a small temperature drop across the diode (i.e., a high k_f). In the reverse mode (Fig. 3(b)), the heat transfer was essentially blocked, leading to a much larger temperature drop (i.e., a low k_r).

Like many phase-change systems, our thermal diode in the forward mode has a variable thermal conductance dependent on the vapor temperature (Fig. 4). The vapor temperature, taken as the average between the superhydrophobic condenser and the superhydrophilic evaporator, was varied with the heat sink temperature (10, 25, and 40 °C) in conjunction with the heater power (30–90 W) for all three system orientations. The forward conductivity exhibited an exponential increase with the vapor temperature, attaining a maximum of $k_f = 44 \pm 12$ W/m·K during the week-long test. The main source of uncertainty was the ±0.1 °C interchangeability of each thermistor, resulting in a conservative uncertainty of ±0.2 °C for ΔT.[16]

The effective conductivity in the reverse mode was taken as the value measured at room temperature, $k_r = 0.29 \pm 0.06$ W/m·K, where the uncertainty was assessed from multiple measurements at all three orientations with a fixed $T_0 = 25$ °C.[16] Other heat sink temperatures were not used because thermal leakage to the environment distorted the measurements of such a low conductance. Note that the

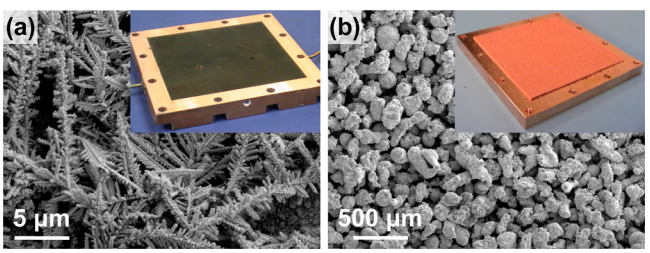

FIG. 2. (Color online) Scanning electron images of (a) the superhydrophobic surface with galvanically deposited micro/nano structures and (b) the superhydrophilic surface with sintered copper wick. Insets: the corresponding copper plates.

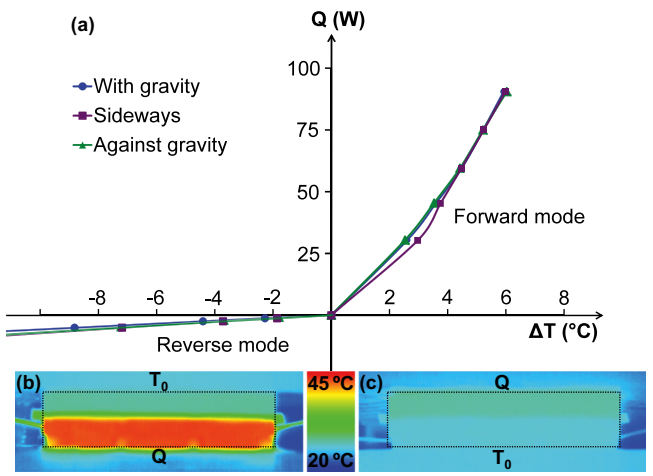

FIG. 3. (Color online) Orientation-independence of the diode performance. (a) All three orientations were tested on the same chamber with the heat sink held at 25 °C. (b) and (c) Infrared imaging of the diode at steady-state in the reverse and forward modes, respectively. The diode (outlined by a dotted box) had an overall dimension of $76 \times 76 \times 18$ mm^3. For both images, the cold side was attached to a heat sink at $T_0 = 25$ °C, while the other side was heated by a resistive film with $Q = 15$ W. Note that the insulating spacer slightly protruded from the sides. The injection and vacuum ports were connected to the superhydrophobic plate, located at the bottom in both cases.

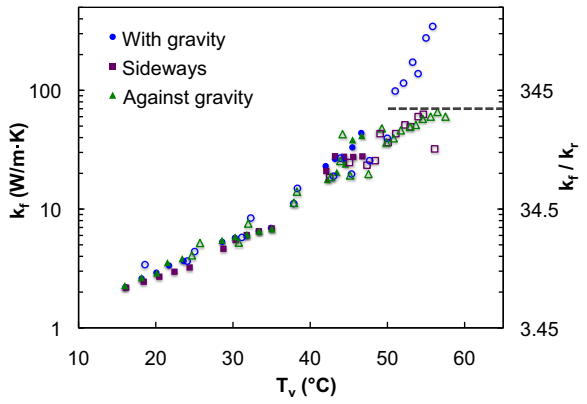

FIG. 4. (Color online) Semi-log plot of the forward thermal conductivity (k_f) versus the average vapor temperature of the thermal diode (T_v). For the corresponding conductivity ratio (k_f/k_r), the reverse conductivity is assumed constant at $k_r = 0.29$ W/m·K. Solid symbols correspond to measurements obtained during a week-long continuous run while open symbols represent additional tests. When $T_v < 50$ °C, the forward conductivity was approximately independent of orientation for heater powers (Q) ranging from 30 W to 90 W. When $T_v > 50$ °C, however, the forward conductivity had a strong orientation dependence, where the "with gravity" orientation yielded much higher values than the other two for a low power of 30 W chosen to delay dryout. The orientation dependence beyond a vapor temperature of 50 °C indicated the onset of boiling, where the removal of vapor bubbles was strongly dependent on the gravitational orientation. The dashed line corresponds to the maximum forward conductivity (k_f^m) predicted by Eq. (2), assuming no enhancement by boiling.

effective reverse conductivity was higher than the thermal conductivity of any of the interstitial materials (mainly vapor and rubber), indicating that the reverse heat transfer was not only through conduction but also through convection.

During the week-long continuous test, a nominal diodicity of up to $\eta = 150 \pm 50$ was measured. Higher forward conductivities and diodicities were measured with additional tests at higher vapor temperatures, but under those conditions, boiling within the wick had likely occurred, which was indicated by the loss of orientational independence with $T_v > 50$ °C. At low heat fluxes, the vapor bubbles could readily escape by buoyancy at the "with gravity" orientation but not at the other two orientations.[17] The boiling limit was corroborated by the sudden loss of wick superhydrophilicity due to dryout, after which the wick had to be rejuvenated.

Near the boiling limit, phase-change heat transfer is very effective such that the majority of the temperature drop on the entire diode is across the wick. Assuming no enhancement by boiling, the maximum forward conductivity is given by

$$k_f^m \approx k_w \frac{A_w H}{H_w A} = k_w \frac{A_w}{A}\left(1 + \frac{H_v}{H_w}\right), \qquad (2)$$

which serves as an upper bound for the *orientation-independent* forward conductivity. In Fig. 4, the conductivity at the "sideways" and "against gravity" orientations reached a plateau of 66 W/m·K, consistent with $k_f^m \approx 70$ W/m·K for $H/H_w = 2.6$ as predicted by Eq. (2). With a thinner rubber gasket ($H = 1.4$ mm) under otherwise identical conditions, the plateau value was 43 W/m·K, consistent with $k_f^m \approx 40$ W/m·K for $H/H_w = 1.4$.

The thermal diode design adopted here may be further optimized. According to Eq. (2), the maximum forward conductivity (and overall diodicity) can be enhanced by minimizing the thickness of the wick structure (H_w) while maximizing the vapor space (H_v). However, there exists an upper limit for H_v beyond which the condensate cannot jump back to the superhydrophilic wick against gravity and/or the opposing vapor flow. To completely understand the physics governing the jumping-drop diode (including the H_v limit), the dynamics and distribution of the dropwise condensate need to be studied in an evacuated chamber, which is expected to deviate from the measurements in open air.[11] For the proof of concept, we used a monolayer thiol coating for the superhydrophobic surface which is known to be unstable at temperatures above 70 °C or so. If a higher working temperature is desired, alternative coatings (e.g., silane) may be used. Since our diode is completely enclosed, the monolayer coating may be more durable compared to an open system, which must be established by long-term tests including those on the effects of the jumping drops.

In summary, we have developed a planar jumping-drop thermal diode that retains the large diodicity of phase-change diodes with the additional advantages of orientational independence and large-area scalability. The two-dimensional diode is expected to be particularly useful for the cooling of planar electronic components such as microprocessors, especially in thermally hostile environments and three-dimensional (layered) microsystems. The scalable design is perfect for large-area applications, such as solar panels for energy harvesting and adaptive walls for the thermal management of buildings.

This work was supported by a DARPA Young Faculty Award (Contract No. N66001-10-1-4048) with A. Bar-Cohen and T. Kenny as technical mentors. We thank F. Liu for assistance in the infrared imaging.

[1]M. Groll, W. Munzel, and W. Supper, J. Spacecr. Rockets **16**, 195 (1979).
[2]A. Mohamad, Sol. Energy **61**, 211 (1997).
[3]S. Varga, A. Oliveira, and C. Afonso, Energy Build. **34**, 227 (2002).
[4]L. Wang and B. Li, Phys. World **21**, 27 (2008).
[5]P. O'Callaghan, S. Probert, and A. Jones, J. Phys. D **3**, 1352 (1970).
[6]C. Chang, D. Okawa, A. Majumdar, and A. Zettl, Science **314**, 1121 (2006).
[7]W. Kobayashi, Y. Teraoka, and I. Terasaki, Appl. Phys. Lett. **95**, 171905 (2009).
[8]D. Reay and P. Kew, *Heat Pipes*, 5th ed. (Butterworth-Heinemann, Oxford, 2006).
[9]J. Perkins, UK Patent No. 7059 (1836).
[10]C. Chen, Q. Cai, C. Tsai, C. Chen, G. Xiong, Y. Yu, and Z. Ren, Appl. Phys. Lett. **90**, 173108 (2007).
[11]J. Boreyko and C. Chen, Phys. Rev. Lett. **103**, 184501 (2009).
[12]J. Boreyko and C. Chen, Phys. Fluids **22**, 091110 (2010).
[13]D. Quere, Rep. Prog. Phys. **68**, 2495 (2005).
[14]I. Larmour, S. Bell, and G. Saunders, Angew. Chem., Int. Ed. **46**, 1710 (2007).
[15]The copper wick was sintered by Thermacore, Inc.
[16]The systematic errors in both temperature and power measurements were smaller than the error bars reported here. The actual power input (Q) was affected by the thermal leakage by conduction through the foam and convection and radiation from the uninsulated sidewalls. The thermal leakage was negligible in the forward mode but could be up to 15% of the total power in the reverse mode. The measured temperature drop (ΔT) included that on the 2 mm interspace between the superhydrophobic (superhydrophilic) surface and the respective thermistor. This undesired temperature drop was negligible in the reverse mode but could be as much as 0.05 °C (considering the two interspaces) with a power of 30 W in the forward mode.
[17]A. Faghri, *Heat Pipe Science and Technology* (Taylor & Francis, New York, 1995).